Geomechanics and Engineering, *Vol. 37, No. 5 (2024) 511-525*
https://doi.org/10.12989/gae.2024.37.5.511

Reinforcement effect of micropile and bearing characteristics of micropiled raft according to the cohesion of soil and stiffness of pile

KangIL Lee[1a], MuYeun Kim[2b] and TaeHyun Hwang*[1]

[1]*Department of Civil Engineering, Daejin University, Gyeonggi-do, Korea*
[2]*Department of Technology Research, IWENC. Co. Ltd., Seoul 02055, Korea*

(*Received November 20, 2023, Revised May 12, 2024, Accepted May 13, 2024*)

Abstract. Micropiled raft has been used to support the existing and new structures or to provide the seismic reinforcement of foundation systems. Recently, research on micropile or micropiled raft has been actively conducted as the usage of micropile has increased, and the reinforcement effect of pile for the raft, the pile installation methods, and methods for calculating the bearing capacity of micropiled raft have been proposed. In addition, existing research results show that the behavior of this foundation system is different depending on the pile conditions and can be greatly influenced by the characteristics of the upper or lower ground depending on the conditions of pile. In other words, considering that the micropile is a friction pile, it can be predicted that the reinforcing effect of micropile for the raft and the bearing capacity of micropiled raft may depend on the cohesion of upper soil layer depending on the pile conditions. However, existing studies have limitations in that they were conducted without taking this into account. However, existing studies have limitations as they have been conducted without considering these characteristics. Accordingly, this study investigated the reinforcing effect of micropile and the bearing characteristics of micropiled raft by varying the cohesion of upper soil layer and the stiffness of pile which affect the behavior of micropiled raft. In this results, the reinforcing effect of micropile on the raft also increased as the cohesion of soil layer increased, but the reinforcing effect of pile was more effective in ground conditions with decreased the cohesion. In addition, the relationship between the axial stiffness of micropile and the bearing capacity of micropiled raft was found to be a logarithmic linear relationship. It was found that the reinforcing effect of micropile can increase the bearing capacity of raft by 1.33~ 3.72 times depending on the cohesion of soil layer and the rigidity of pile.

Keywords: cohesion of soil; micropile; micropiled raft; numerical analysis; pile stiffness

1. Introduction

A micropile known as the friction piles with a diameter of 300 mm or less are the small diameter cast in place piles that are installed in the ground through the process of boring a ground, inserting the steel bar, and grouting. When this pile method was first proposed, it was mainly used to reinforce the bearing capacity or to suppress settlement of the existing foundation system as one of the underpinning methods. However, with the development of pile materials in recently, this method has be used for geotechnical purposes such as supporting new structures, securing the stability of slopes or retaining wall structures, and earthquake resistant of structures.

As the usage of micropile increases in field, several researchers conducted studies related to the bearing characteristics of micropiled rafts, pile installation methods, and improvement of the seismic performance of foundation through a model test or numerical analysis (Hwang *et al.* 2019, EI Kamash *et al.* 2020). In addition, the reinforcing effect of micropile for the foundation had been proven through case studies applied in the field (Lopes *et al.* 2020, Wen *et al.* 2020, Wang *et al*. 2021, Elsawwaf *et al.* 2023).

Through existing stydy results, it can be confirmed that the reinforcing effect of the micropile for the raft considerably depends on the installed conditions of piles (diameter or length of micropile), the behavior of the micropiled raft may be different from that of the piled raft. In other words, the stiffness conditions of micropile have a significant impact on the bearing characteristics of micropiled raft, it is not appropriate to evaluate the bearing capacity of the micropiled raft through the design concept of existing piles.

However, most existing studies were limited to the increasing effect of the bearing capacity on the micropiled rafts according to the installed conditions of micropile, and research on the bearing characteristics of micropiled rafts in relation to the stiffness conditions of pile is insufficient.

Micropile is a friction pile, and the behavior of pile shows the behavior characteristics of rigid or flexible pile in the ground depending on the pile installed conditions. In particular, as shown in the research results of Hwang *et al.* (2017), the behavior of micropiled rafts may show behavior similar to that of shallow foundations in the case of flexible pile conditions. Considering the behavior characteristics of micropiled rafts, it can be said that the bearing capacity of micropiled rafts also depends on the conditions of upper soil layer.

*Corresponding author, Adjunct Professor
E-mail: makgoh77@nate.com
[a]Professor
[b]Ph.D.

ISSN: 2005-307X (Print), 2092-6219 (Online)

The cohesion of soil is generated by capillary bonding even in silt or sandy ground, not clay (Shin 2016). In addition, the ground targeted for pile construction may be a cohesive granular soil layer containing more than 15% of clay content since the ground on site is very diverse, and it can be said that not only the particle roughness but also the cohesion of soil affects the skin friction of pile (Potyondy and Eng 1961, Khanmohammadi and Fakharian 2018 Wang *et al.* 2020, Zhuang *et al.* 2023).

Therefore, the cohesion of upper soil layer can be said to be a major factor that affect the bearing capacity of micropiled raft. However, existing studies have focused only on the study on the reinforcement effect of micropile according to the cross sectional change of pile without considering the characteristics for the cohesion of upper soil layer.

This study performed the field compression test for prototype micropile and 3D numerical analysis that simulated the test process, and evaluated the feasibility of researching micropile rafts through numerical analysis by comparing the field test and numerical analysis results. And, this study performed an additional 3D numerical analyses on the micropiled raft to evaluate the reinforcing effect of micropile and the bearing capacity of foundation system according to the cohesion of upper soil layer and the stiffness conditions of pile.

In this results, the reinforcing effect of micropile on the raft also increased as the cohesion of soil layer increased, but the reinforcing effect of pile was more effective in ground conditions with decreased the cohesion. In addition, when considering the cohesion of soil layer, the relationship between the axial stiffness of micropile and the bearing capacity of micropiled raft was found to be a logarithmic linear relationship, and the relationship between the axial stiffness ratio and the bearing capacity of micropiled raft was found to be a linear relationship.

2. Mcropiled raft system

2.1 Micropiled raft

A micropile refers to a small diameter pile composed of steel bars and grout, as shown in Fig. 1, and the application of micropile within the foundation of a structure is generally determined by considering the load conditions on the foundation and the ground conditions beneath the foundation. This foundation type is called the micropiled raft (Fig. 2). This foundation system is divided into vertical micropiled raft and inclined micropiled raft, and the vertical micropiled raft type is mainly applied in field because it is easy to construct piles in the vertical direction. The design of micropiled rafts is generally performed by evaluating whether the bearing capacity of micropile is secured by applying the existing design concept of deep foundation.

2.2 Bearing characteristics of micropiled raft

As the usage of micropile has increased, research on micropiled rafts has been conducted through various

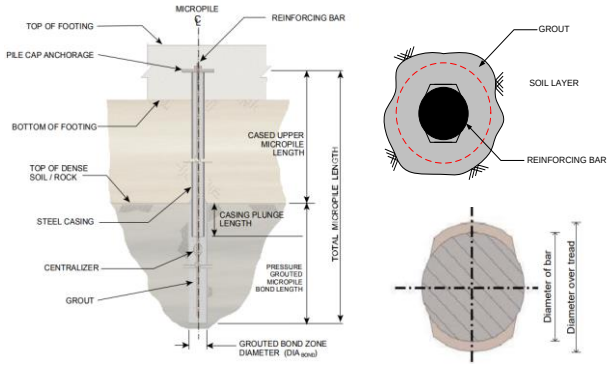

Fig. 1 Structure of micropile (FHWA 2005)

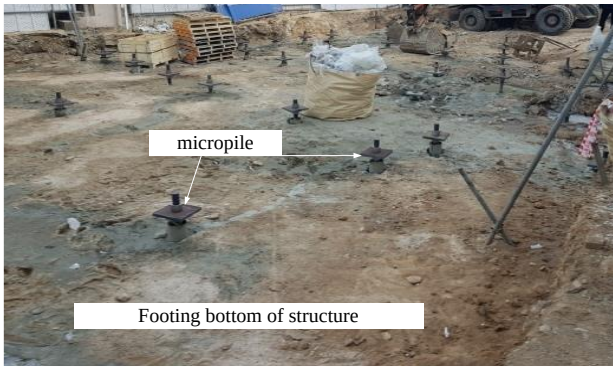

Fig. 2 Installation of micropiles in footing

research methods such as numerical analysis and model test. And results of existing research related to micropiled raft show that the behavior and bearing capacity of micropiled rafts depends on the stiffness conditions of micropile and ground conditions beneath a foundation.

Han and Ye (2006) conducted a field test to investigate the earth pressure distribution in the ground beneath a micropiled raft before and after micropile reinforcement. And it was shown that the earth pressure increases at the corners of foundation before installing piles, and the earth pressure increases significantly within the ground restrained by the piles after installing piles.

Tsukada *et al.* (2006), Hwang *et al.* (2011), Elwakil and Azzam (2016) and Elsawwaf *et al.* (2022) conducted a study on the bearing characteristics of micropiled raft according to the installation angle of pile through a model test or a numerical analysis. And, in order to effectively reinforce the foundation, the installation of micropile was proposed to be installed vertically in case of the rigid pile condition, and installed at an angle 30° or 45° in case of the flexible pile condition.

Hwang *et al.* (2017) and Azzam and Basha (2018) evaluated the behavior and bearing characteristics of micropiled raft in slender pile conditions through model tests, and showed that the behavior of foundation system significant depends on the ground condition adjacent to the upper pile and the stiffness of pile. In addition, a method forcalculating the bearing capacity of micropiled raft was proposed considering the behavior characteristics of mcicropiled rafts investigated through model tests.

Ebadi-Jamkhaneh and Kontoni (2023) suggested through numerical analysis that the increase of pile length is more effective than increasing the diameter when installing micropiles for foundation reinforcement. And, Elsawwaf *et al.* (2023) proposed through a case study that the settlement of the structure was reduced by 79.9% and 73.9% when reinforcing the micropile foundation, and that the vertical load sharing ratio of the pile was reduced through the ground consolidation process.

Studies have also been conducted on the behavior and bearing characteristics of micropile that support the micropiled raft, and these existing research results show that the bearing capacity of a micropile is mainly influenced by the conditions of the cross section of pile and ground adjacent to the pile. Moradi *et al.* (2021), who studied the bearing properties of micropile through model test, showed that the relative density of ground adjacent to the pile is an important factor in the bearing capacity of pile. Qian *et al.* (2014) proposed that the interpreted failure loads or capacities under tension are 66-87% of those under compression in case of the micropiles in loess under in-situ moisture content through field test.

Jang and Han (2018) showed that the bearing capacity of micropile with a wave-shaped surface of pile increased by 1.4-2.3 times compared to the existing micropile through field tests. As suggested by Shamy *et al.* (2020), the increase in pile length can be said to be limited due to the increase in the foundation fixation and the buckling ratio of pile. Hwang *et al.* (2022) suggested through field compression tests of micropile conducted at 6 sites that the total settlement of micropile significantly depends on the change in diameter of steel bar that are components of the pile.

EI Kamash *et al.* (2017), Wang *et al*. (2019), and Capatti *et al*. (2020) also conducted studies on the seismic effect of micropile, it was suggested that that the seismic performance of pile is greatly influenced by the stiffness conditions of micropile structure. Lupattelli *et al*. (2023) studied the behavior of micropiled rafts under repeated thermal loading conditions through numerical analysis, it was suggested that significant settlement of the foundation system occurs because the resistance of the micropile shaft decreases in the initial cooling cycle due to the shrinkage of the micropile and the interaction of pile-adjacent soil.

3. Behavior characteristics of micropile

3.1 Soil conditions and micropile specifications

Fig. 3 shows the ground conditions and the specifications of micropile at the urban railway site where compression tests were performed to investigate the behavior characteristics of micopile. The ground conditions confirmed from the field ground investigation were the landfill layer, the weathered soil layer and the weathered rock layer. The thickness of landfill layer and weathered soil layer respectively were 4 m and 12 m, and it was investigated that the weathered rock layer beneath the soil layer was very highly fractured state (N≥50/10). In addition, in the case of the ground density investigated through the standard penetration test(SPT), the landfill was loose or medium sand layer with N = 5/30~10/30($N_{ave.}$=7), the weathered soil was medium or very dense sandy soil layer with N=13/30~48/30 ($N_{ave.}$=30).

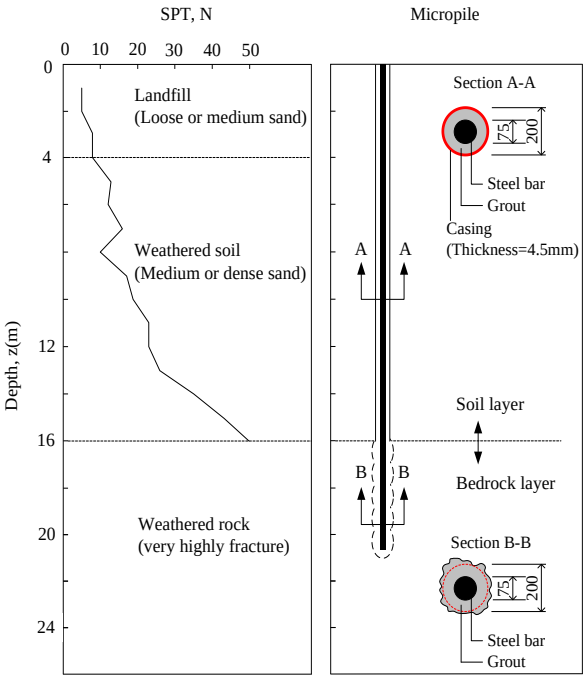

Fig. 3 Ground conditions and micropile in field test

The diameters of the micropile and steel bar (D or d_{ST}) and the installation length (L) of pile were determined considering the magnitude of working load(P_W) on the pile head, and the magnitude of working load considered in design was 400 kN (P_W=400 kN). And the diameters of micropile and steel bar were 200 mm and 75 mm (D=200 mm; d_{ST}=75 mm) and the installation length of pile was 21m, as shown in Fig. 3.

The installation of micropile was carried out in the following order: boring the ground, inserting the casing and steel bar and grouting, as shown in Fig. 4. The casing with a thickness of 4.5 mm was installed within the soil layer to prevent the collapse of the bored hole during pile construction.

3.2 Field compression test of micropile

Fig. 5 shows that the field compression test performed for the prototype micropile installed in the field. The field test was conducted in accordance with the testing process proposed by FHWA (2005). As shown in Fig. 5, the test load was applied to the head of the pile using a hydraulic jack, and the load cell and electronic dial gauge were used to measure the load and displacement of pile during the test. The magnitude of test load at each stage was the total load divided into 4 steps (0.5 P_W, 1.0 P_W, 1.5 P_W, and 2.0 P_W), and the loading or unloading process was repeatedly performed at each step during the test.

The load was maintained for the duration until the displacement of the pile converged after applying the load

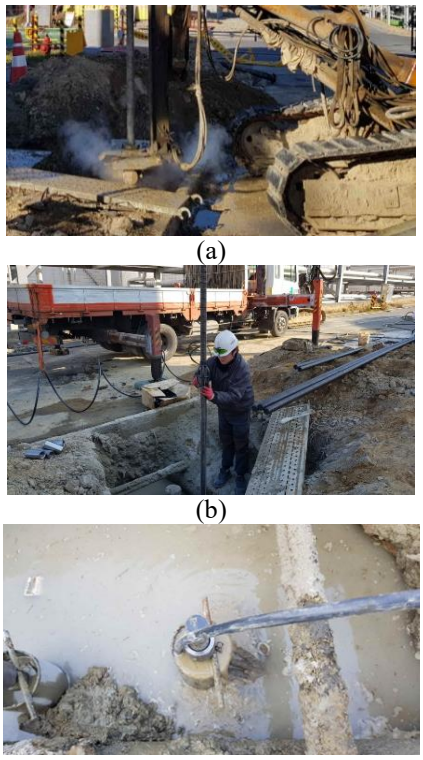

(a) (b) (c)

Fig. 4 Construction of micropile : (a) ground boring, (b) insertion of casing and steel bar, and (c) grouting in the bored hole

Fig. 5 Field compression test of micropile

at each step, and the test load of the next step was applied after the displacement of the pile converged. The magnitude of the test load(P_T) at the final test stage was 940 kN (P_T=940 kN≥2·PW=2×400=800 kN), more than twice the working load (P_W=400 kN).

3.3 Numerical model of micopile

Fig. 6 shows a numerical model simulating the field test process to evaluate the behavioral characteristics of micropile. The program used in this study is MIDAS NX (Ver. 3.40), which is used for design and research in the field of geotechnical engineering. The size of the numerical model was 60 m×25 m (diameter × height, m).

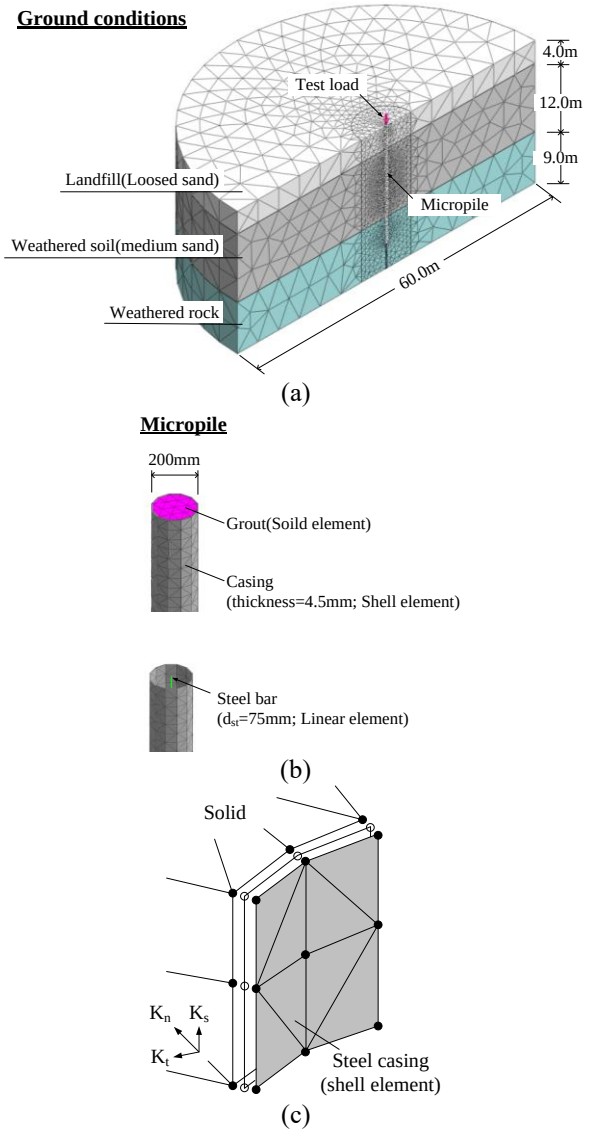

Fig. 6 Numerical model to estimate the behavior of micropile ; (a) 3D model, (b) structure of micropile, and, and (c) interface of ground/casing

The ground conditions of numerical model were a landfill layer (loose sand), a weathered soil layer (medium density sand), and a weathered rock layer, as shown in Fig. 6. The thicknesses of landfill layer and weathered soil layer were 4.0 m and 12.0 m, respectively. The thickness of the weathered rock layer was determined considering the boned length of pile (L_{BL} = 5.0 m; Fig. 3) and the influence range of pile tip (= 4D or more; Das, 2011). The thickness of the weathered rock layer determined in this way was 9.0 m. And the diameters of micropile and steel bar were 200mm and 75mm, identical to the specifications of test pile.

The ground elements were modeled as the tetrahedral solid elements. As shown in Fig. 6, the ground elements were formed densely in the case of elements adjacent to the pile (size of element=0.15 m), and loosely formed in the case of elements adjacent to the boundary of model (size of element= 4.0 m). The numerical elements of micropile were

Table 1 Input data in numerical analysis

Classification	$N_{ave.}$	γ (kN/m³)	E (MPa)	μ	c' (kPa)	φ' (°)	Analysis model
Landfill sand	7	15.0	7.0	0.25	0	25°	Mohr-coulomb's model
Weathered soil (medium dense sand)	30	17.0	30	0.30	0	30°	
Weathered rock	50	19.62	60	0.35	10	35°	
Steel bar	-	78.5	210,000	0.35	-	-	Elastic model
Grout	-	23.5	23,200	0.175	-	-	
Concrete	-	23.5	71,500	0.175	-	-	

Note: Elastic modulus of soil, E_S=1,000 N(sand) or 1,200 N(weathered rock); FHWA(2005)
Elastic modulus of grout, $E_G=\sqrt{4{,}732\sigma_{ck}}$(MPa), where σ_{ck}=24 MPa ; FHWA(2005)
Elastic modulus of concrete(raft) : $E_C=8{,}500\sqrt[3]{\sigma_{ck}}$, where σ_{ck}=20 MPa(MPa) ; KR(2014)

a beam element in case of steel bar, a shell element in case of casing (thickness=4.5 mm), and a tetrahedral solid element in case of grout. Since the material stiffness difference between the ground and the casing is large, the interface effect (zero thickness interface element) was considered for the boundary condition of the ground/casing, as suggested by Day and Potts (1994) and Shin (2015).

The zero thickness interface elements were adopted to consider the interface behavior between the casing and the ground by defining the vertical stiffness K_s, the normal stiffness K_n, and shear stiffness K_t to the shell axis, as shown in Fig. 6(c). The stiffness values are automatically set by the program based on the material properties (MIDAS 2010). The calibration factors for the interface stiffness are evaluated as follows

$$K_s \gg G_s = \frac{E_s}{2(1+\mu_s)} \tag{1}$$

$$K_t = K_n = \frac{2(1-\mu_s)}{1-2\mu_s} \cdot K_s \gg \frac{2(1-\mu_s)}{1-2\mu_s} \cdot \frac{E_s}{2(1+\mu_s)} \tag{2}$$

Where, E_S and G_S are the elastic and shear modulus of soil, and μ_S means the poisson's ratio of soil.

The load condition was a line load condition, and it was applied on the head of steel bar (beam element) as shown in Fig. 6(a). The magnitude of total load was 1,000 kN ($P_{final\ step} \geq 2.5P_W$=1,000 kN) which is 2.5 times the working load, and the magnitude of load applied for each analysis step was 100 kN (ΔP=100 kN). The unit weight (γ), elastic modulus (E), poisson's ratio (μ), cohesion and shear resistance angle (c' and φ'), and yield model of material applied to the numerical model are shown in Table 1.

These input values are the results of field ground investigation and design values applied to micropile design (FHWA 2005, KR 2014). The yield model of ground was Mohr-Coulomb's model, and the associated flow rule was applied to simulate the plastic behavior of pile. This considers the characteristics of pile that exhibit the bearing capacity even when the small plastic deformation of ground occurs, as shown in Fig. 8. In addition, this study evaluated the behavior of micropile using an analysis model modeled according to the procedure shown in Fig. 7.

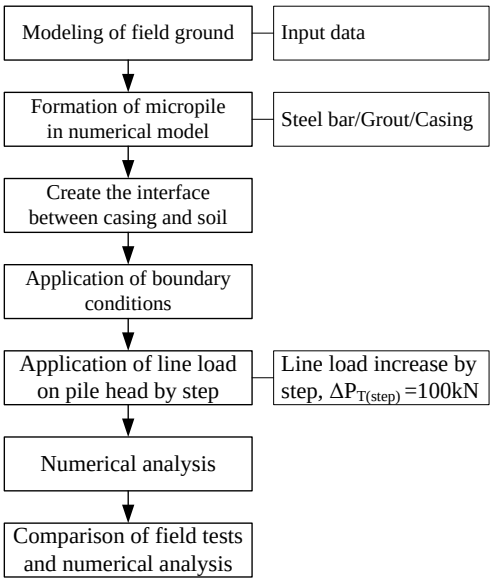

Fig. 7 Process of numerical analysis

3.4 Behavior of micopile

Fig. 8 shows the results of numerical analysis simulating the field test process, and the behavior of the micropile was investigated as the displacement concentrated in the upper part of pile and the ground adjacent to the pile as the load increased.

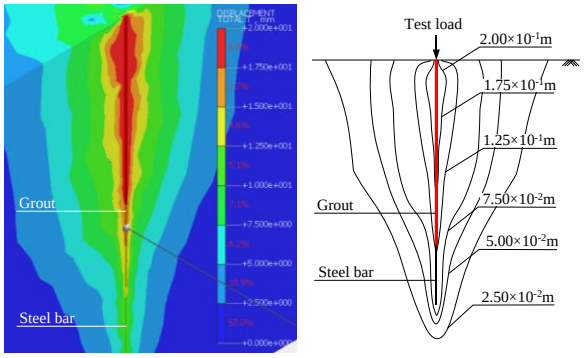

Fig. 8 Behavior of micropile through numerical analysis

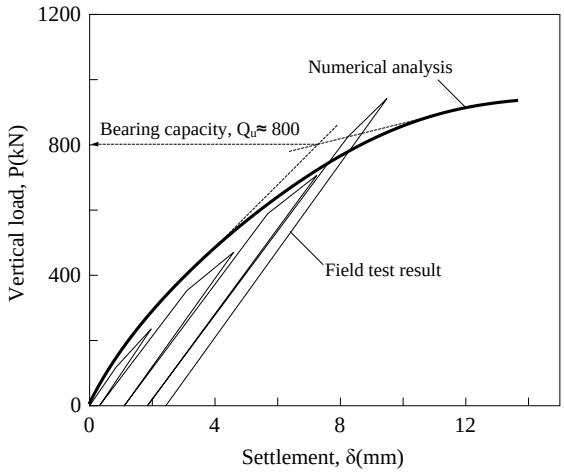

Fig. 9 Comparison of the load-settlement relationship in field test and numerical analysis

Fig. 9 compares the load-displacement relationship of micropile investigated through field test and numerical analysis. The bearing capacities of the piles investigated through field tests and numerical analysis were 940 kN and 800 kN when pile displacement is 9.5 mm, and the two results were similar. In other words, these comparison results shows that there is no problem in simulating the behavior of micropile in the ground or studying the behavior and bearing characteristics of micropiled raft through numerical analysis.

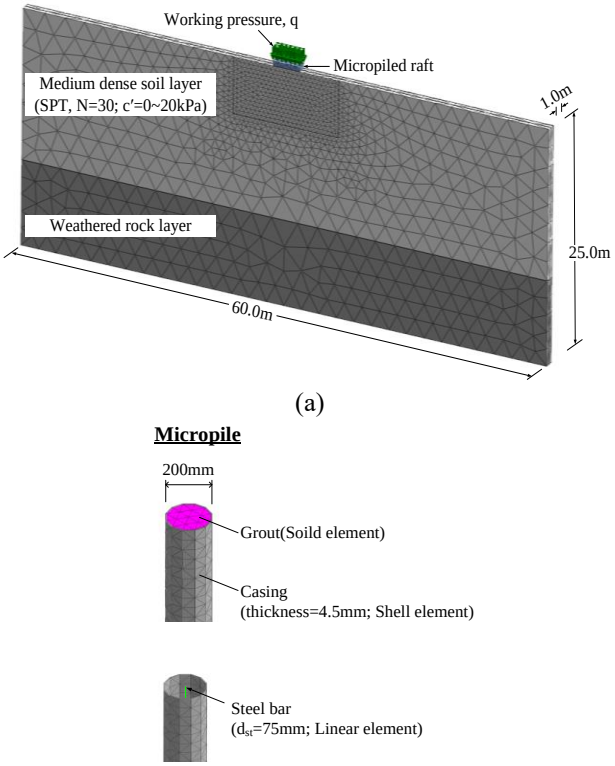

Fig. 10 Numerical model to estimate the bearing capacity of micropiled raft: (a) numerical model, and (b) micropiled raft

4. Bearing capacity of micropiled raft

4.1 Numerical model and analysis conditions

The stability evaluation of foundation systems such as a spread foundations or piled rafts is generally performed with the design concept of a 2D continuous foundation with a unit length of 1.0 m. However, the micropile is a pile composed of steel and grout with different stiffness (Fig. 1), unlike conventional piles (concrete piles and steel piles, etc.) constructed with a single material. Therefore, a 2D analysis model is not suitable for simulating the behavior of a micropiled raft. In addition, an analysis model that can simulate the behavior of micropiled raft by applying different stiffness of pile to meet the purpose of study will be required. Accordingly, this study performed 3D numerical analysis on rafts and micropiled rafts with a unit length of 1.0 m, as shown in Fig. 10.

Fig. 10 shows a 3D numerical model to evaluate the bearing characteristics of micropiled raft. The size of numerical model is 60.0 m × 1.0 m × 25.0 m (width × length × height, m), as shown in Fig. 10(a). The ground conditions were a soil layer and a weathered rock layer, since the bearing layer considered for micropile in design is mainly a rock layer with the strength of weathered rock. Therefore, in this study, the ground conditions of numerical model for the behavior and bearing characteristics of micropiled raft were soil and weathered rock layers. As suggested by Elsawwaf *et al*. (2023), the load transfer characteristics of micropiles in the foundation system may differ depending on the consolidation process of soil layer. However, the consolidation process of the soil layer was not considered in this study, because piles are generally installed in ground that has been consolidated.

Considering that the soil layer in field is mainly a medium density sand layer as shown in Fig.6(a), the soil layer of 3D numerical model was modeled as a medium density sand layer ($N_{ave.}$ = 30). And the thickness of the soil layer was 16.0 m, the same thickness as Fig. 6(a). Since the cohesion of soil (c) is a major factor related to the bearing capacity of foundation system and the skin friction of micropile, the cohesion of soil layer was applied differently from 0.0 to 20.0 kPa, as shown in Fig. 10(a).

The ground element was a tetrahedral solid element, the elements adjacent to raft and micropile formed densely (element size = 0.5 m or less), and the elements adjacent to the boundary of model formed loosely (element size = 2.5 m). The boundary condition applied to the bottom of model was a fixed condition that constrained vertical, horizontal, and rotational displacements.

And the boundary condition applied to the side of model was the constraint condition of lateral and longitudinal displacement. The size (width × length × thickness, m) of raft, which is a component of the micropiled raft, was 3.0×1.0×0.5 m as shown in Fig. 10(b), and it was modeled as a tetrahedral solid element (element size=0.5 m).

Table 2 Conditions of micropiled raft in numerical analyses

Model type	c'(kPa)	Micropile conditions			
		Length, L(m)	Space, s(m)	Dia. of pile, D (mm)	Dia. of bar, d_{st} (mm)
Raft(R)	0, 10, 20	-	-	-	-
Micropiled raft(MR)	0	21	2.5(s≥4D)	100, 200, 300	10, 30, 50, 75
	10	21	2.5(s≥4D)	100, 200, 300	10, 30, 50, 75
	20	21	2.5(s≥4D)	100, 200 ,300	10, 30, 50, 75
	30	21	2.5(s≥4D)	100, 200 ,300	10, 30, 50, 75

This raft corresponds to a rigid foundation with the stiffness index (K_r) of 1 or more obtained through Eq. (3) ($K_r \approx 19.69$; Das 1983). The load condition on the foundation was a uniform load condition as shown in Fig. 10(a), and the magnitude of working pressure(Δq) increased for each analysis step was 20 kN/m^2 (Δq=20 kN/m^2)

$$K_r = \frac{1}{6}\left(\frac{1-\mu_s^2}{1-\mu_F^2}\right)\left(\frac{E_F}{E_s}\right)\left(\frac{T}{b}\right)^3 \quad (3)$$

Where, μ_S and μ_F is the poisson's ratio of the ground and foundation, and E_S and E_F is the elastic modulus of ground and foundation. And T is the thickness of foundation, and b means 1/2 of the width of foundation.

The modeling of micropile was the same as the modeling process of the numerical model simulating the field test, as shown in Fig. 6. The grout was a solid element, the steel bar was a beam element, and the casing was a shell element.

The total length of micropile(L) was modeled as 21.0m, the same as the length of the test pile shown in Fig. 3 and 6, and the length of pile embedded in the weathered rock layer was 5.0 m(L_{BL}=5.0 m). In general, designers place piles at installing space of 2.0 to 2.5 m in the footing, taking into account the allowable space between piles of 3.0D or more, and interference between micopiles during construction (KGS 2018, Ahmed *et al.* 2023). Therefore, as shown in Fig. 10(b), the foundation width (B=3.0 m) and the spacing of micropile were determined in the study, and the spacing of piles in the foundation was 2.50 m.

The diameters of micropile and steel bar usually installed in field are 100 to 300 mm and 19 to 75 mm, respectively (FHWA 2005, Elsawwaf *et al*. 2022). Considering these, the total diameter of micropile was 100~300 mm, and the diameter of steel bar was 10~75 mm. In this study, the bearing capacity of raft and micropiled raft was evaluated for each analysis conditions in Table 2, and the bearing capacity of foundation system was determined by the working pressure when the allowable settlement was 25 mm.

4.2 Behavior and bearing capacity of foundation system

Fig. 11 shows the ground displacement of raft and micropiled raft predicted through numerical analysis when the settlement (δ) of foundation system relative to the foundation width (B) occurs more than 10% (at failure, δ/B≥10%). The notation of foundation system for each condition are presented in Table 3, refer to them.

As shown in Figs. 11(a)-11(c), the ground displacement was concentrated within the soil layer supporting the foundation and extended to the ground surface adjacent to the foundation, in the case of R(0), R(10) and R(20). In addition, as the cohesion of upper soil layer increased, it was found that the displacement zone of ground was further expanded. In other words, these results show that the soil layer with increased cohesion more effectively resists the load transferred from the raft, and that the cohesion of soil layer is a major factor affecting the bearing capacity of foundation system.

The ground displacement of micropiled raft investigated for each conditions was also found to expand the zone of ground displacement as the cohesion of soil layer increased. As shown in Figs. 11(e) and 11(f), in the case of a micropiled raft with pile and steel bar diameters of 100 mm and 75 mm, the ground displacement was concentrated in the soil restrained by the micropile. And the zone of ground displacement was expanded, as the cohesion of soil increased. It was observed that the displacement zone of ground restrained by the micropile expanded even under the conditions of D=200 mm and 300 mm, as shown in Figs. 11(g) and 11(h), Figs. 11(k) and 11(l).

The ground displacement of the micropiled raft according to changes in the diameter of pile and steel bar showed the characteristic that the ground displacement occurred only within the soil layer when the diameter of steel bar was small. However, as the diameter of pile and steel bar increased, the ground displacement of foundation system showed that the displacement was concentrated within the ground restrained by the piles and transferred to the weathered rock layer. In particular, the zone of ground displacement expanded by increasing the diameter of the pile was found to be larger than that caused by the increase in cohesion of soil layer.

As shown in Fig. 11(d), the ground displacement of micropiled raft showed that the ground displacement was concentrated in the upper soil layer and transferred to the ground surface adjacent to the foundation, when the

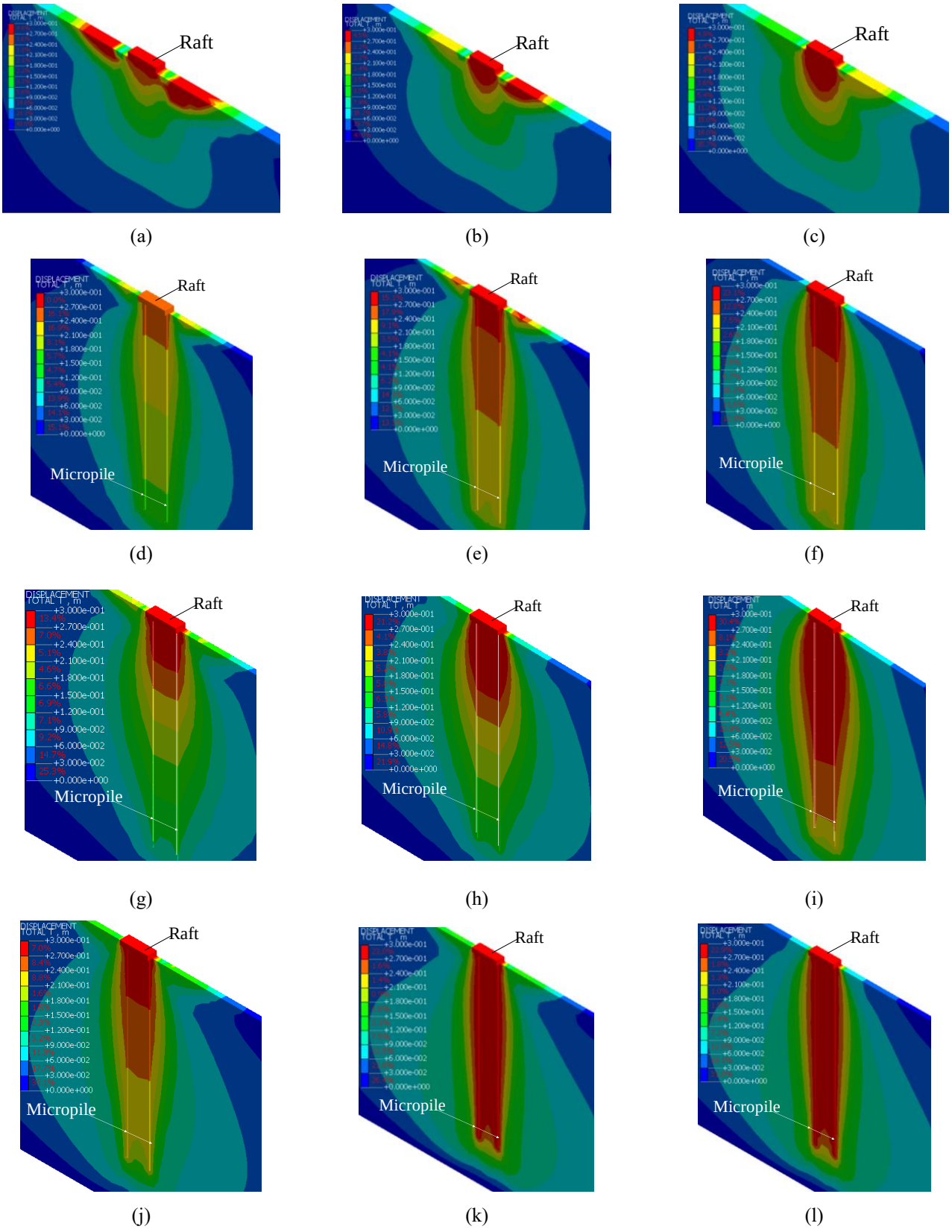

Fig. 11 Ground displacement of foundation system at failure: (a) R(0), (b) R(10), (c) R(20), (d) MR(100-30-0), (e) MR(100-75-0), (f) MR(100-75-20), (g) MR(200-10-0), (h) MR(200-10-20), (i) MR(200-75-0), (j) MR(300-30-0), (k) MR(300-75-0), and (l) MR (300-75-10)

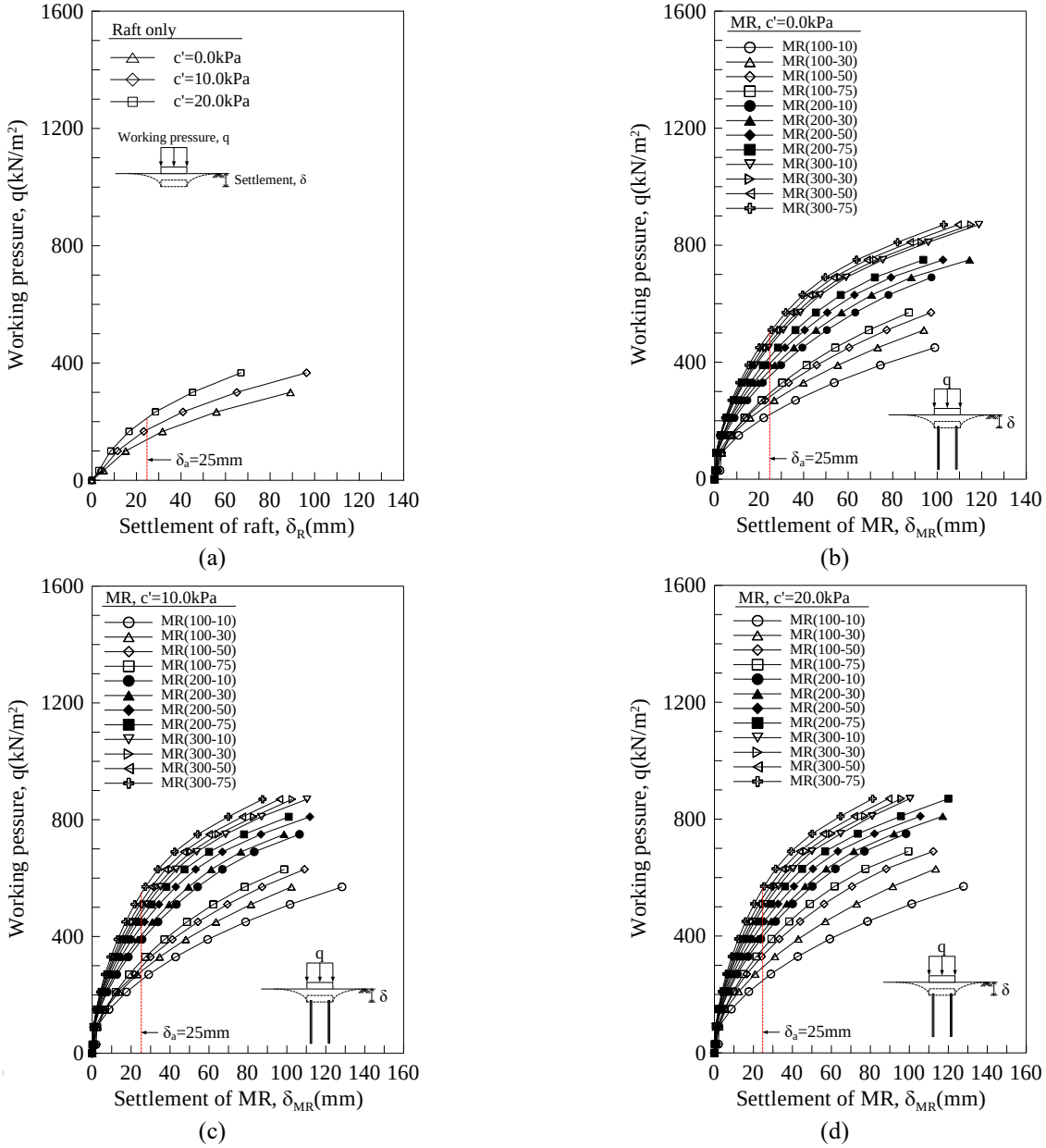

Fig. 12 Load-displacement relationship of foundation system; (a) raft only, (b) MR in case of c′=0.0 kPa, (c) MR in case of c′=10.0 kPa, and (d) MR in case of c′=20.0 kPa

diameters of pile and steel bar were 100 mm and 30 mm and the cohesion of soil layer was 0.0kPa. Similar behavior characteristics could be confirmed under the condition that the diameters of the pile and the steel bar are 200 mm and 10 mm and the cohesion of soil layer is 0.0 kPa (Fig. 11(g)).

However, in the case of the behavior of micropiled raft with the pile diameter increased from 100 mm to 300 mm, the zone of displacement in the ground restrained by the pile extended to the bottom of the pile, as shown in Figs. 11(d) and 11(j). In addition, even when only the diameter of the steel bar was increased, the failure area within the ground restrained by the pile was expanded (Figs. 11(e) and 11(f), Figs. 11(j) and 11(k)).

In other words, these results show that changes in pile diameter have a significant impact on the behavior and bearing capacity of micropiled rafts. It shows that the bearing capacity of micropiled raft can depend on the characteristics of upper ground when the pile diameter is small, and it can depend on the characteristics of hard lower ground when the pile diameter is large.

Fig. 12 shows the relationship of working pressure-settlement for each foundation system investigated through numerical analysis results. When the settlement amount of foundation system occurred was same, the resistance pressure of raft increased as the cohesion of soil layer increased (Fig. 12(a)). And the resistance pressure of micropiled raft also increased as the diameter of micropile and steel bar increased (Figs. 12(b)-12(d)).

The study results shown in Fig. 12 provide the basic data that can be used to consider the effect of increasing the

Table 3 Bearing capacity of foundation system for each condition

Classification	c'(kN/m^2)	Micropile		q_a (kN/m^2)	Notation
		D (mm)	d_{st} (mm)		
Raft	0	-	-	140	R(0)
	10	-	-	171	R(10)
	20	-	-	207	R(20)
Micropiled raft	0	100	10	220	MR(100-10-0)
			30	241	MR(100-30-0)
			50	270	MR(100-50-0)
			75	288	MR(100-75-0)
	10	100	10	246	MR(100-10-10)
			30	267	MR(100-30-10)
			50	296	MR(100-50-10)
			75	315	MR(100-75-10)
	20	100	10	276	MR(100-10-20)
			30	298	MR(100-30-20)
			50	327	MR(100-50-20)
			75	348	MR(100-75-20)
	0	200	10	360	MR(200-10-0)
			30	381	MR(200-30-0)
			50	407	MR(200-50-0)
			75	436	MR(200-75-0)
	10	200	10	381	MR(200-10-10)
			30	403	MR(200-30-10)
			50	430	MR(200-50-10)
			75	460	MR(200-75-10)
	20	200	10	403	MR(200-10-20)
			30	426	MR(200-30-20)
			50	452	MR(200-50-20)
			75	483	MR(200-75-20)
	0	300	10	460	MR(300-10-0)
			30	474	MR(300-30-0)
			50	500	MR(300-50-0)
			75	525	MR(300-75-0)
	10	300	10	478	MR(300-10-10)
			30	492	MR(300-30-10)
			50	518	MR(300-50-10)
			75	547	MR(300-75-10)
	20	300	10	497	MR(300-10-20)
			30	512	MR(300-30-20)
			50	540	MR(300-50-20)
			75	569	MR(300-75-20)

Note: R(cohesion): Raft condition by a cohesion
MR(dia.of micropile−dia. of steel bar-cohesion) : Micropiled raft condition by the dia. of pile and cohesion

bearing capacity or reducing settlement of foundation system.

This study can evaluate the effect of reducing settlement of the foundation system according to the conditions of the ground and pile, but considered the bearing capacity of foundation system corresponding to 25 mm of allowable settlement to meet the study purpose.

Table 3 summarizes the bearing capacity, q_a, of the foundation system for each condition investigated through the results in Fig. 12. Where, the bearing capacity of the foundation system for each condition is the working pressure corresponding to the settlement of 25.0 mm investigated through the relationship of pressure-settlement in Fig. 12.

4.3 Bearing characteristics of foundation with the cohesion of soil layer

Fig. 13 compares the bearing capacity of foundation system for each condition according to the change in cohesion of soil layer. As shown in the figure, as the cohesion increased in all conditions, the bearing capacity of raft and micropiled raft also increased. As shown in Fig. 13(a), the bearing capacity of raft was 141.0~197.0 kPa, and the bearing capacity of micropiled raft for each condition was 220.0~348.0 kPa when the total diameter of pile was 100 mm.

The bearing capacity of micropiled raft was about 360.0~ 483.0 kPa when the total diameter of pile was 200mm, and the bearing capacity of micropiled raft was 460.0~569.0 kPa when the total diameter of pile was 300mm, as shown in Figs. 13(b) and 13(c). Additionally, the bearing capacity of micropiled raft was maximum in case of c=20.0 kPa, D=300 mm, and d_{ST}=75 mm.

Fig. 14(a) compares the increase in bearing capacity (Δq_a) of the foundation system for each condition according to the increase in cohesion ($\Delta c'$) under the same ground conditions. However, the increase in the bearing capacity of micropiled raft according to the increase in cohesion was relatively decreased compared to the pile diameter of 100 mm when the pile diameter was 200 mm or more.

The reason why the increase in bearing capacity of foundation system differs depending on the increase in cohesion can be predicted through the behavior characteristics of raft and micropiled raft in Fig. 11. The behavior of raft observed through numerical analysis shows that ground displacement is concentrated in the soil layer beneath the foundation and extends to the adjacent ground of the foundation, as shown in Fig. 11(a) to 11(c). In other words, it can be said that the bearing capacity of raft depends on the characteristics of upper soil layer. Similar behavior characteristics were also observed in the behavior of micropiled rafts when the pile diameter was small (case of D=100 mm; Figs. 11(d) and 11(e)).

On the other hand, the micropiled raft behavior shows that displacement is concentrated within the ground restrained by the pile, and the failure zone extends to the weathered rock layer when the pile diameter is large(D≥ 200 mm; Figs. 11(i), 11(k) and 11(l)). These results mean that the load working on the pile head is transmitted to the hard lower ground, and that the micropiled raft is relatively less affected by the characteristics of upper soil layer than when the pile diameter is small as the pile diameter increases. In other words, the bearing capacity of micropiled raft depends on the strength characteristics of upper soil layer when the pile diameter is small, whereas the bearing capacity depends on the change in the stiffness of pile when the pile diameter is large(case of D≥200 mm, in this study).

Fig. 14(b) compares the bearing capacity ratio of foundation system (BCR), which is the bearing capacity of raft divided by the bearing capacity of micropiled raft for each condition, as shown in Eq. (4). These results provide evaluation data on the reinforcing effect of micropile for the

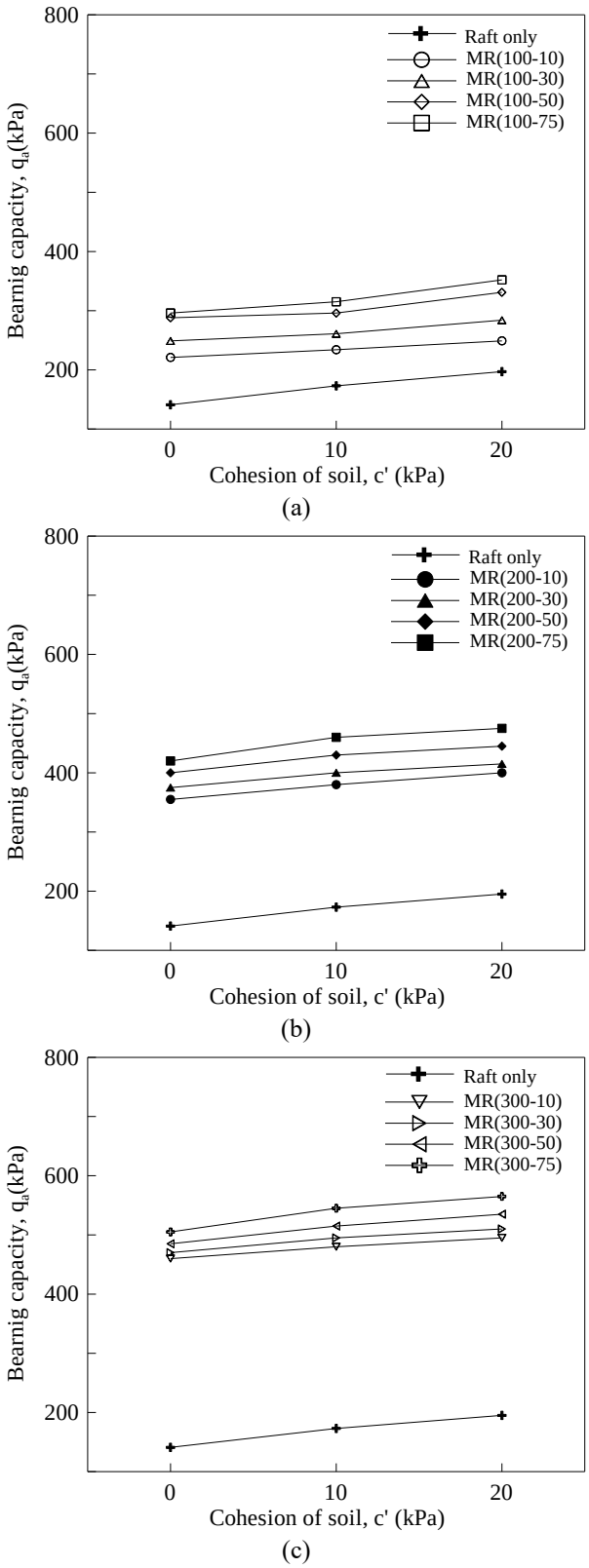

Fig. 13 Bearing capacity and BCR of foundation system according to the cohesion of soil; (a) D=100 mm, (b) D=200 mm, and (c) D=300 mm

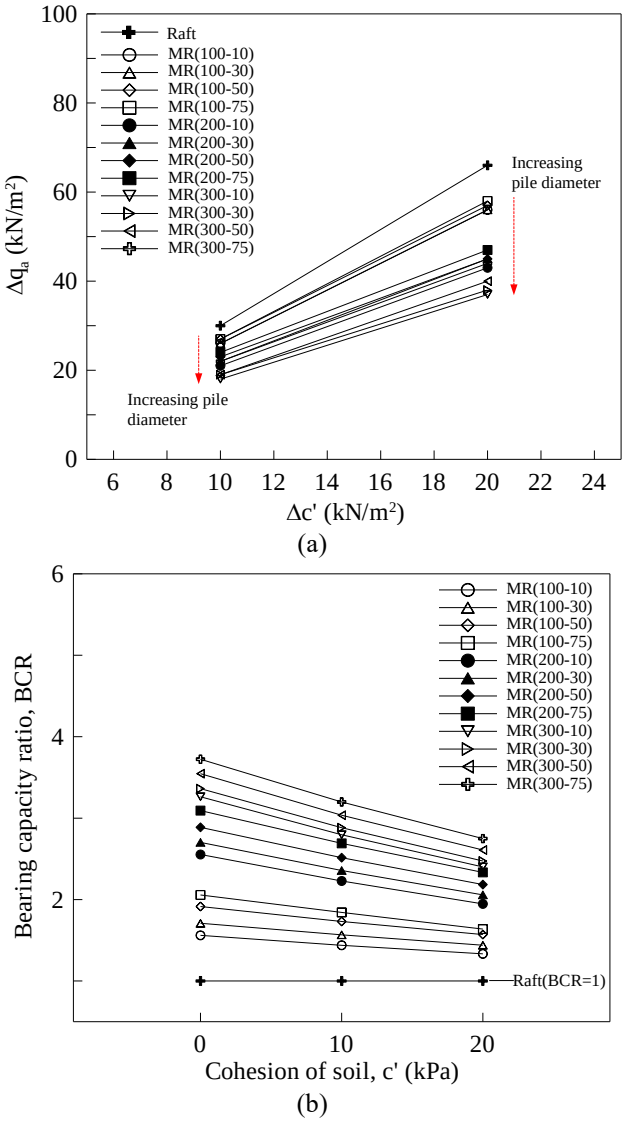

Fig. 14 $\Delta c' - \Delta q_a$ and BCR of foundation system according to the cohesion of soil layer: (a) $\Delta c' - \Delta q_a$, and (b) BCR according to the cohesion of soil layer

foundation according to changes in cohesion of upper soil layer

$$\text{Bearing capacity ratio, BCR} = \frac{q_{a-MR}}{q_{a-R}} \quad (4)$$

Where, $q_{a\text{-}R}$ and $q_{a\text{-}MR}$ mean the bearing capacity of the raft and micropiled raft for each condition under the same ground conditions, the bearing capacity ratio of raft is 1.0 when calculated through Eq. (4) (BCR_{raft} = 1.0).

As shown in Fig. 14(b) the bearing capacity ratio, BCR, of the foundation system according to the change in cohesion of the soil layer was 1.33~3.72, and BCR was the maximum at 3.72 in case of c'=0.0 kPa, D=300 mm, and d_{ST}=75 mm. And, the BCR was found to be 2.75 in the case of the same diameter and c'=20.0 kPa, which was rather decreased compared to the BCR in the case of c'=0.0 kPa. The reasons for this can be confirmed through the results in Fig. 14(a).

First, it was found that the increase in the raft's bearing capacity due to the increase in cohesion was the largest among all foundation systems. On the other hand, as the pile diameter increased, it was found that the increase in bearing capacity of foundation system was smaller than that of the raft and the foundation systems with small diameter. This can be said to be due to the behavior characteristics (Fig. 11) where the bearing capacity of the micropiled raft is less affected by the characteristics of the upper soil layer as the pile diameter increases. In addition, these comparative results show that the reinforcing effect of micropile for raft can be expected to increase the bearing capacity by up to 3.72 times, and that pile reinforcement is more effective in ground without the cohesion of soil layer.

4.4 Bearing characteristics of foundation with the axial stiffness of pile

In design of pile, the axial stiffness of micropile (E_PA_P) is calculated as Eq. (5) considering the pile structure in Fig. 1 (FHWA 2005). And this factor is a design value used to predict the elastic displacement of the pile structure.

$$E_PA_P = E_{ST}A_{ST} + E_GA_G \quad (5)$$

Where, E_P and A_P are the elastic modulus and cross-sectional area of micropile ($=\pi D^2/4$). E_{ST} and A_{ST} are the elastic modulus and cross-sectional area($=\pi d_{st}^2/4$) of steel bar, and E_G and A_G are the elastic modulus (Table 1) and cross-sectional area($=\pi D^2/4 - A_{ST}$) of grout.

The results in Figs. 11 and 14 show that the behavior and bearing characteristics of micropiled raft depend more on the change in the diameter of micropile than on the cohesion of soil layer. This can be said to be because micropiles in the ground show the behavior of flexible or rigid pile depending on the diameter of pile, and the behavior of micropiled raft shows behavior similar to shallow or deep foundation because of the behavior characteristics of pile. Therefore, an investigation on the bearing capacity of micropiled raft in relation to the stiffness conditions of pile will be required.

Fig. 15 compares the bearing capacity of micropiled raft according to the diameter of the micropile and the axial stiffness of the pile. As shown in Fig. 15(a), the bearing capacity of the micropiled raft was 220~339 kPa in case of pile diameter 100 mm, the bearing capacity was 360~ 483 kPa in case of pile diameter 200 mm, and the bearing capacity was 460~569 kPa in case of pile diameter 300 mm. In addition, the bearing capacity of micropiled raft tended to increase nonlinearly with increasing the axial stiffness of pile(E_PA_P) considering the material properties and cross sectional area of pile, as shown in Fig. 15(b).

Fig. 16 compares the relationship between $\log_{10}[q_{a\text{-}MR}]$-$\log_{10}[E_PA_P]$ for each conditions investigated through the results in Fig. 15(b). The bearing capacity of micropiled raft tends to increase logarithm-linearly with increasing the axial stiffness of pile as shown in Fig. 16, and the relationship between the axial stiffness of pile and the bearing capacity of micropiled raft obtained approximately through this was as follows

$$log_{10}[q_{a-MR}] \approx 0.34 \cdot log_{10}[E_PA_P] + 0.57 \quad (6)$$

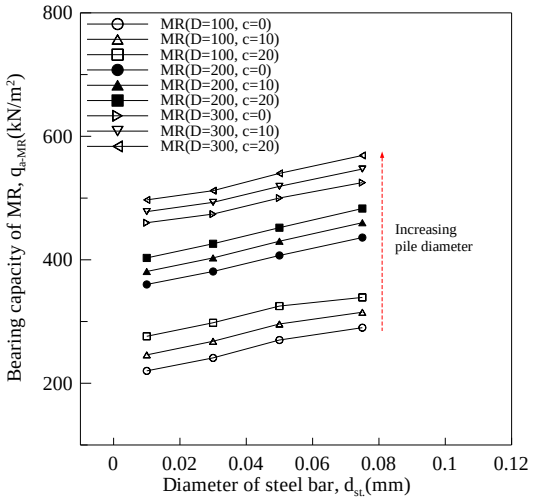

Fig. 15 Bearing capacity of foundation system according to the diameter and axial stiffness of micropile; (a) $q_{a\text{-}MR}$ according to D and d_{ST}, and (b) $q_{a\text{-}MR}$ according to E_PA_P

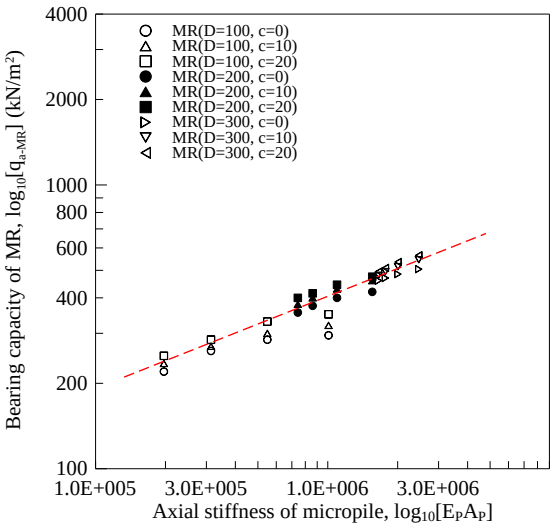

Fig. 16 Relationship of $\log_{10}[q_{a\text{-}MR}]$ and $\log_{10}[E_PA_P]$

Micropile shows the characteristic that the steel bar supports the transferred load firstly and then transfers it to the grout and ground (FHWA 2005). This is due to the difference in stiffness of materials that compose the pile, and the axial stiffness of steel bar can be said to be a very important factor when considering the load transfer characteristics of pile. Accordingly, this study investigated the relationship between the axial stiffness ratio of pile ($E_{ST}A_{ST}/E_PA_P$) and the bearing capacity of micropiled raft ($q_{a\text{-}MR}$).

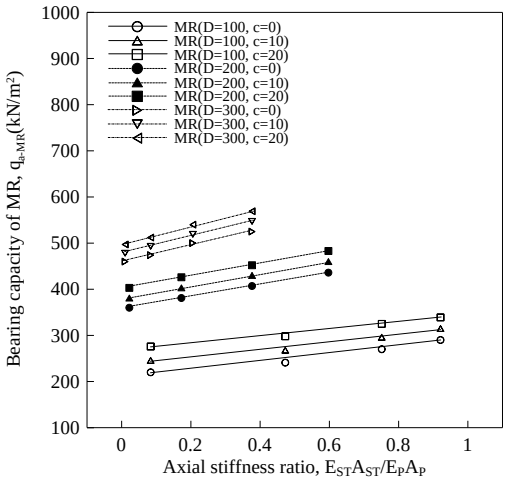

Fig. 17 $q_{a\text{-}MR}$ according to $E_{ST}A_{ST}/E_PA_P$

Table 4. Coefficient a and b in Eq. (7)

Dia. of micropile	c'(kPa)	a	b
D=100 mm	0	80.95	214
	10	82.14	239
	20	85.71	269
D=200 mm	0	131.03	357
	10	136.21	378
	20	137.93	400
D=300 mm	0	175.68	458
	10	186.49	476
	20	194.59	495

Fig. 17 compares the bearing capacity of micropiled raft for each condition according to the axial stiffness ratio of pile. The bearing capacity of micropiled raft for each conditions tended to increase linearly with increasing the axial stiffness ratio, as shown in Fig. 17. In addition, the relationship between $E_{ST}A_{ST}/E_PA_P$ and $q_{a\text{-}MR}$ investigated from the research result in Fig. 17 was as shown in Eq. (7), and the coefficients a and b according to the cohesion of upper soil layer were as shown in Table 4.

$$q_{a-MR} = a \cdot \frac{E_{ST}A_{ST}}{E_PA_P} + b \tag{7}$$

5. Design considerations

The results in Fig. 14(b) show that the reinforcing effect of micropile for the raft varies depending on the cohesion of upper soil layer and the pile diameter, and that the

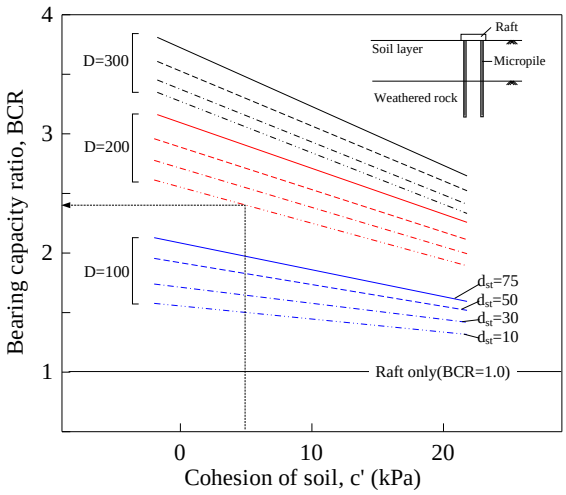

Fig. 18 Foundation reinforcement effect of micropile (BCR of foundation system)

reinforcing effect of pile can be quantitatively evaluated. This is because the behavior of micropiled rafts varies depending on the pile diameter and may or may not be greatly affected by the characteristics of upper soil layer (Fig. 11).

Fig. 18 presents the reinforcing effect of micropile for raft based on the research results in Fig. 14(b), and the reinforcing effect under conditions not considered in this study can be predicted through these results. For instace, if the cohesion of upper soil layer is 15 kPa and the diameters of micropile and steel bar are 200 mm and 10 mm respectively, the reinforcing effect of micropile for the raft is approximately 2.4 times ($BCR_{MR(200\text{-}10\text{-}15)}\approx 2.4$).

The results in Figs. 16 and 17 show that the bearing capacity of a micropiled raft is greatly dependent on the axial stiffness of pile and the axial rigidity ratio, and has a linear relationship between the axial stiffness of pile and the axial stiffness ratio. As a results of reviewing the Eqs. (6) and (7) proposed through these relationships, Eq. (6) can estimate the bearing capacity of micropiled raft considering the axial stiffness of pile, but cannot consider the cohesion of upper soil layer.

In other words, it provides only approximate bearing capacity of micropiled raft. On the other hand, Eq. (7) can consider the axial stiffness of pile and the cohesion of upper soil layer, which affect the bearing capacity of the foundation system. And, it can also calculate the bearing capacity of the foundation system under conditions not considered in this study. Fig. 19 shows the changes in coefficients a and b of Eq. (7) based on the results in Table 4, it will be possible that the bearing capacity of micropiled raft can be obtained in more detail than the results of Eq. (6) by using Eq. (7) and Fig. 19.

6. Conclusions

This study performed numerical analysis and field tests to evaluate the reinforcing effect of micropile and the supporting characteristics of micropile raft according to the diameter of pile (steel bar) and the cohesion of soil layer. As a result of the study, the behavior and bearing capacity of the micropiled raft were found to be more affected by the stiffness condition of pile rather than the cohesion of soil layer, and the detailed study results are as follows.

- The behavior and bearing capacity of micropiled raft depended on the property of upper soil layer when the stiffness of micropile was small, and on the property of hard lower ground when the stiffness of pile was large.
- The reinforcing effect of micropile for the raft was up to 3.72 times, and the reinforcement of pile was more effective in the upper soil layer without cohesion when the reinforcing effect of micropile was evaluated by varying the cohesion of upper soil layer and the stiffness of pile.
- The relationship between the stiffness of pile(E_PA_P) and the bearing capacity of micropiled raft($q_{a\text{-}MR}$) was found to be a logarithmic linear relationship ($\log_{10}[E_PA_P] \propto \log_{10}[q_{a\text{-}MR}]$).
- The relationship between the axial stiffness ratio($E_{ST}A_{ST}/E_PA_P$) and thhe bearing capacity of micropiled raft($q_{a\text{-}MR}$) was found to be a linear relationship ($E_{ST}A_{ST}/E_PA_P \propto q_{a\text{-}MR}$).

This conclusion could provide a design guide for predicting the bearing capacity of micropile rafts in the preliminary design stage. However, the results of this study can be said to be limited as they are based on the condition of the foundation width of 1.0 m, and additional study considering various spacing conditions of pile is necessary.

References

Ahmed, D., Bttaib, S.N.L., Ayadat, T. and Hasan, A. (2022), "Numerical analysis of the carrying capacity of a piled raft foundation in soft clayey soils", *Civil Eng. J.*, **8**(4), 622-636. https://doi.org/10.28991/CEJ-2022-08-04-01.

Azzam, W.R. and Basha, A.M. (2018), "Utilization of micro-piles for improving the sub-grade under the existing strip foundation: experimental and numerical study", *Innov. Infrastruct. Solutions*, **3**, 1-11. https://doi.org/10.1007/s41062-018-0149-0.

Capatti, M.C., Dezi, F., Carbonari, S. and Gara, F. (2020), "Dynamic performance of a full-scale micropile group relevance of nonlinear behaviour of the soil adjacent to micropiles", *Soil Dyn. Earthq. Eng.*, **128**, 105858. https://doi.org/10.1016/j.soildyn.2019.105858.

Das, B.M. (1983), Advanced Soil Mechanics (International Edition), McGraw-Hill, Washington, DC, USA.

Das, B.M. (2011), Principle of Foundation Engineering (7th Ed.), Cengage Learning, Boston, Massachusetts, USA.

Day, R.A. and Potts, D.M. (1994), "Zero thickness interface elements numerical stability and application", *Int. J. Numer. Anal. Method. Geomech.*, **18**(10), 689-708. https://doi.org/10.1002/nag.1610181003.

Ebadi-Jamkhaneh, M. and Kontoni, D.P.N. (2023), "Static analysis of prestressed micropile-raft foundation with varying lengths resting on sandy soil", *Innov. Infrastruct. Solut.*, **8**(3), 106. https://doi.org/10.1007/s41062-023-01076-y.

El Kamash, W. and Han, J. (2017), "Numerical analysis of existing foundations underpinned by micropiles", *Int. J. Geomech.*, **17**(6), 04016126. https://doi.org/10.1061/(ASCE)GM.1943-5622.0000833

El Kamash, W., El Naggar, H., Nabil, M. and Ata, A. (2020),

"Optimizing the unconnected piled raft foundation for soft clay soils: numerical study", *J. Civil Eng. - KSCE*, **24**(4), 1095-1102. https://doi.org/10.1007/s12205-020-0567-3.

Elsawwaf, A., Nazir, A. and Azzam, W. (2022), "The effect of combined loading on the behavior of micropiled rafts installed with inclined condition", *Environ. Sci. Pollut. Res.*, **29**, 81321-81336. https://doi.org/10.1007/s11356-022-21327-2/

Elsawwaf, A., El Sawwaf, M., Farouk, A., Aamer, F. and El Naggar, H. (2023), "Restoration of tilted buildings via micropile underpinning: A case study of a multistory building supported by a raft foundation", *Buildings*, **13**(2), 422, https://doi.org/10.3390/buildings13020422.

Elwakil, A.Z and Azzam, W.R. (2016). "Experimental and numerical study of piled raft system", *Alexandria Eng. J.*, **55**(1), 547-560. https://doi.org/10.1016/j.aej.2015.10.001.

Elsawwaf, A., El Sawwaf, M., Nazir, A., Azzam, W., Farouk, A. and Etman, E. (2023), "Consolidation effect on the behavior of micropiled rafts under combined loading: Case study", *Arabian J. Sci. Eng.*, **48**(10), 13429-13448. https://doi.org/10.1007/s13369-023-07806-9.

FHWA (2005), "Micropiles design and construction", US Department of Transportation, Washington, DC, USA.

Han, J. and Ye, S.L. (2006), "A field study on the behavior of a foundation underpinned by micropiles", *Can. Geotech. J.*, **43**(1), 30-42. https://doi.org/10.1139/t05-087.

Hwang, E.P., Yang, W.Y. and Lee, K.I. (2019), "Reinforcement effect of micropile according to the pile section change", *J. Korean Soc. Hazard Mitigation*, **19**(2), 185-195. https://doi.org/10.9798/KOSHAM.2019.19.2.185.

Hwang, T.H. and Kwon, O.Y. (2011), "Installation methods of micropiles by the length ratio of pile and the depth of rock layer", *J. Korean Geotech. Soc.*, **27**(4), 5-20. https://doi.org/10.7843/kgs.2011.27.4.005.

Hwang, T.H., Kim, K.H. and Shin, J.H. (2017), "Effective installation of micropiles to enhance bearing capacity of micropiled raft", *Soils Found.,* **57**(1), 36-49. https://doi.org/10.1016/j.sandf.2017.01.003.

Hwang, T.H., Cho, J.M. and Lee, Y.S. (2022), "Calculation method for settlement of micropile installed in rock layers through field tests", *Geomech. Eng.*, **31**(2), 197-208. https://doi.org/10.12989/gae.2022.31.2.197.

Jang. Y.E. and Han, J.T. (2018), "Field study on axial bearing capacity and load transfer characteristic of waveform micropile", *Can. Geotech. J.*, **13**, 653-665. https://doi.org/10.1139/cgj-2017-0155.

KGS (2018), "Structure foundation design standards and commentary", Korean Geotechnical Society, Korea.

Khanmohammadi, M. and Fakharian, K. (2018), "Evaluation of performance of piled-raft foundations on soft clay: A case study", *Geomech. Eng.*, **14**(1), 43-50. https://doi.org/10.12989/gae.2018.14.1.043.

KR (2014), "KR C-10010 Concrete bridge design principles and materials", Korea national railway(KR), Korea.

Lopes, F.R., D'Hyppolito, L.C.B.S., Danziger, F.A.B. and Becker, L.B. (2020), "Settlements during underpinning with different processes: Case of a hospital in Rio de Janeiro, Brazil", *J. Geotech. Geoenviron. Eng.*, **146**(6), https://doi.org/10.1061/(ASCE)GT.1943-5606.0002266.

Lupattelli, A., Bourne-Webb, P.J, Freitas, T.M.B. and Salciarini, D. (2023), "A numerical study of the behavior of micropile foundations under cyclic thermal loading", *Appl. Sci.*, **13**(17), https://doi.org/10.3390/app13179791.

MIDAS (2010), "Manual of MIDAS GTS: Application Method and Input Material Properties of Interface Element", MIDAS IT, Korea.

Moradi, M.H., Keramati, M., Ramesh, A. and Naderi, R. (2021), "Experimental valuation of the effects of structural parameters installation methods and soil density on the micropile bearing capacity", *Int. J. Civil Eng.*, **19**(11), 1313-1325. https://doi.org/10.1007/s40999-021-00629-5.

Potyondy, J.G. and Eng, M. (1961), "Skin Friction between Various Soils and Construction Materials", *Géotechnique*, **11**(4), 339-353. https://doi.org/10.1680/geot.1961.11.4.339.

Qian, Z.Z. and Lu, X.L., Yang, W.Z. and Cui, Q. (2014), "Behaviour of micropiles in collapsible loess under tension or compression load", *Geomech. Eng.*, **7**(5), 477-493. http://dx.doi.org/10.12989/gae.2014.7.5.477.

Shamy, E.N., Ahmed, S.M. and Abdel-Motaal, M.A. (2020), "Seismic response of multi-story structure strengthened with micropiles", *Int. J. Eng. Adv. Tech.*, **9**(6). https://doi.org/10.35940/ijeat.f1511.089620.

Shin, J.H. (2015), "Geomecanics & Engineering: behavior and modelling", CIR, Seoul, Korea.

Tsukada, Y., Miura, K., Tsubokawa, Y., Otani, Y. and You, G. (2006), "Mechanism of bearing capacity of spread footings reinforcing with micropiles", *Soils Found.*, **46**(3), 367-376. https://doi.org/10.3208/sandf.46.367.

Wang, C., Han, J.T. and Jang, Y.E. (2019), "Experimental investigation of micropile stiffness affecting the underpinning of an existing foundation", *Appl. Sci.*, **9**(12), 2495. https://doi.org/10.3390/app9122495.

Wang, C., Han, J.T., Kim, S.J. and Jang, Y.E. (2021), "A novel preloading method for foundation underpinning for the remodeling of an existing building", *Geomech. Eng.*, **24**(1), 29-42. https://doi.org/10.12989/gae.2021.24.1.029.

Wen, L., Kong, G., Abuel-Naga, H., Li, Q. and Zhang, Z. (2020), "Rectification of tilted transmission tower using micropile underpinning method", *J. Perform. Constr. Fac.*, **34**(1), https://doi.org/10.1061/(ASCE)CF.1943-5509.0001398.

Zhuang, Y., Hu, S. and Fun, H. (2023), "Bearing capacity of foundation and soil arching in rigid floating piled embankments: Numerical study", *Appl. Sci.*, **13**(18), 10296. https://doi.org/10.3390/app131810296.

CC